



Mn^{II} Location and Adsorbate Interactions in (M)MnH-SAPO-34 and (W)MnH-SAPO-34 studied by EPR and Electron Spin Echo Modulation Spectroscopies

Gernho Back*, Yanghee Kim, Young-Soo Cho and Yong-Il Lee

*Department of Chemistry, Changwon National University, Changwon, Kyungnam, 641-773, Korea

Received October 5, 2002

Abstract: Manganese-doped H-SAPO-34 samples were prepared by an ion-exchanged reaction between H-SAPO-34 and paramagnetic Mn(II) species in methanol media and characterized by ESR and Electron Spin-Echo Modulation(ESEM) studies. In the hydrated (W)MnH-SAPO-34 measured in water, the Mn(II) ion was octahedrally coordinated with four framework oxygens and two water molecules at a displaced site IV of the eight membered ring window in the ellipsoidal cavity, while the Mn(II) ion was octahedrally coordinated to three framework oxygens and three water molecules at a displaced site I' of the six membered ring window in the ellipsoidal cavity in hydrated(M)MnH-SAPO-34 measured in methanol. The similar result was found in the experiments with methanol adsorbents except ethanol.

INTRODUCTION

Various microporous crystalline aluminophosphates(AIPO_{4-n}) have been synthesized hydrothermally with morpholine being used as the templating agent.¹⁻³ A serious defect of these materials with respect to catalytic potential is the lack of Brønsted acidity due to the neutrality of their framework.¹ However, this can be overcome by the substitution of P and/or Al with silicon in their framework to generate negative charged frameworks, yielding the silicoaluminophosphate molecular sieves abbreviated as SAPOs. Isothermal substitution of several different elements into the AIPO_{4-n} framework can be possible, which the framework substitution of phosphorus by silicon is of particular importance for their applications such as adsorbents for separation and purification of molecular sieves, catalyst supports, and ion-exchange agents.⁴ Mn(II) and Co(II) have been incorporated into the chabazite-like structure SAPO-34 and the activity and shape selectivity of these materials were tested on methanol dehydration.⁵

*To whom : ghback@sarim.changwon.ac.kr

In this work, we report a successful synthesis of manganese ion exchanged silicoaluminophosphate-based microporous molecular sieve MnH-SAPO-34 in deionized water and MeOH media, which has the thermally stable chabazite-like structure. The location of the Mn²⁺ ion is characterized by electron paramagnetic resonance (EPR) and electron spin echo modulation (ESEM) spectroscopy to evaluate the coordination environment of Mn(II) in silicoaluminophosphate-34(SAPO-34) molecular sieve clearly.

EXPERIMENTAL SECTION

Synthesis and Solid-state ion exchange of SAPO-34 were carried out by a modification of the reported methods in the literature.⁶ An aqueous solution (4.5 ml) of 85 % H₃PO₄(Mallinckrodt) was prepared by diluting the solution with 6.7 ml of de-ionized water and stirred for 10 min. After adding 7.7 ml of de-ionized water to the H₃PO₄ solution with continuous stirring, four portions (0.175 g for each time) of 0.7 g of Al₂O₃.H₂O (Vista Chemical) were added successively every hour. The resulting homogeneous mixture was followed by successive addition of 0.20 g of fumed SiO₂ (Cab-O-Sil total 0.8 g fumed SiO₂) every 30 min over 2 h periods. Then, the mixture was cooled in ice water and 13.9 ml of triethylamine (Aldrich) was added dropwise followed by continuous stirring at room temperature. The solution was stirred overnight to give a bulk mole ratio of Si₁Al₃P₅. After about 14 h of stirring, the pH of the mixture was adjusted to 6.9 by the addition of 40 wt% HF solution (Aldrich). A Teflon-lined autoclave was filled to 50 % of its capacity with the synthesis mixture and heated to 200 °C and kept for 6 days. The autoclave was then quenched with cold water and the top liquid portion was removed with a pipette followed by washing the crystallized solid product three times with 250 ml of boiling deionized water. Finally the solid product was dried at 110 °C for 12 h in air. This as-synthesized SAPO-34 was analyzed by electron probe microanalysis and had a molar composition of Si_{0.11}Al_{0.55}P_{0.34}. Comparison of X-ray diffraction pattern with that in the literature of the synthesized product showed that the product was single phase with good crystallinity.

Ion-exchanged sample in methanol media denoted by (M)MnH-SAPO-34 was prepared by adding 10 ml of 1 x 10⁻¹ M MnCl₂ to 0.1 g of calcined H-SAPO-34 followed by stirring at 80 °C for 2 h. The ion-exchanged product was then filtered, washed with 20 ml of methanol three times and dried in vacuum desiccator at room temperature for 15 h. The product was ground with a mortar and pestle and pressed in a steel die with about 2 tons for 20 min to make wafers of 12-mm diameter and 2.5-mm thickness. Then pellet was put in a quartz boat and heated in a furnace at 600 °C in O₂ and kept for 15 h. The sample was white and no color change was observed after the ion-exchanged reaction. Since this templating-free MnH-SAPO-34 loses its crystallinity slowly with moisture, samples were stored under vacuum.

The concentration of manganese in MnH-SAPO-34 was calculated from the calibration curve constructed with several standardized MnCl₂ solutions (See Fig. 3). This method is based on the measurement of the quantity of manganese adsorbed on a solid surface for

SAPO-34 molecular by sensing the change in intensity of EPR spectrum obtained by double integration. It was found to be 0.01 mol% for the as-synthesized sample.

Ion-exchanged sample in a de-ionized water denoted (W)MnH-SAPO-34 was prepared by adding 1.7 μl of 1×10^{-1} M $\text{MnCl}_2 \cdot 4\text{H}_2\text{O}$ (Aldrich) to a homogeneous solution, adding 10 ml of de-ionized water to 0.5g calcined H-SAPO-34. The concentration of manganese in (W)MnH-SAPO-34 sample was measured using the same calibration curve method for the (M) MnH-SAPO-34. It was also found to be 0.01 mol% for as-synthesized samples. To acquire a detailed ESEM spectrum for the interaction of Mn(II) ions with water, sample was dehydrated to a temperature of 550 °C, then allowed to be equilibrated with D_2O , CD_3OH , CH_3OD , $\text{CH}_3\text{CH}_2\text{OD}$.

Measurement

The Mn ion-exchange and calcinations of as-synthesized SAPO-34 were examined by the use of a powder X-ray diffraction (XRD) with a Phillips PW 1840 diffractometer. Thermogravimetric analysis was performed by a Dupon 951 thermal analyzer with heating rate of $10 \text{ }^\circ\text{C min}^{-1}$. The EPR spectra were recorded with a modified Varian E-4 spectrometer interfaced to a Tracer Norton TN-1710 signal averager at 77 K. Each spectrum was obtained by multiple scan to achieve a satisfactory signal-to-noise-ratio. Each acquired spectrum was transferred from the signal averager to an IBM PC/XT compatible computer for analysis and plotting. The magnetic field was calibrated with a Varian E-500 gauss meter. ESEM spectrum was measured at 4 K with a Bruker ESP 380 pulsed ESR spectrometer. Three pulse echoes were measured by using a $90^\circ\text{-}\tau\text{-}90^\circ\text{-T-}90^\circ$ pulse sequences with $\tau = 0.26\text{--}0.28 \mu\text{s}$, and echo intensity was measured as a function of T. The theory and simulation of ESEM are described elsewhere.¹⁶

RESULTS

As-synthesized SAPO-34 and MnH-SAPO-34 were well crystallized and X-ray diffraction (XRD) spectra were shown in Fig. 1. There is no significant difference in XRD spectra between as-synthesized SAPO-34 and calcined MnH-SAPO-34. Thermogravimetric analysis shows that as-synthesized SAPO-34 has different weight-losses around 400, 500 and 700 °C, compared to calcined H-SAPO-34 (see Fig. 2). These additional weight losses are probably due to the desorption or decomposition of organic templating agent, triethylamine, which indicates the presence of acid sites. The calcined MnH-SAPO-34 has a weight loss only around 100 °C during heating to the 900 °C. This weight loss is probably due to the desorption of H_2O .

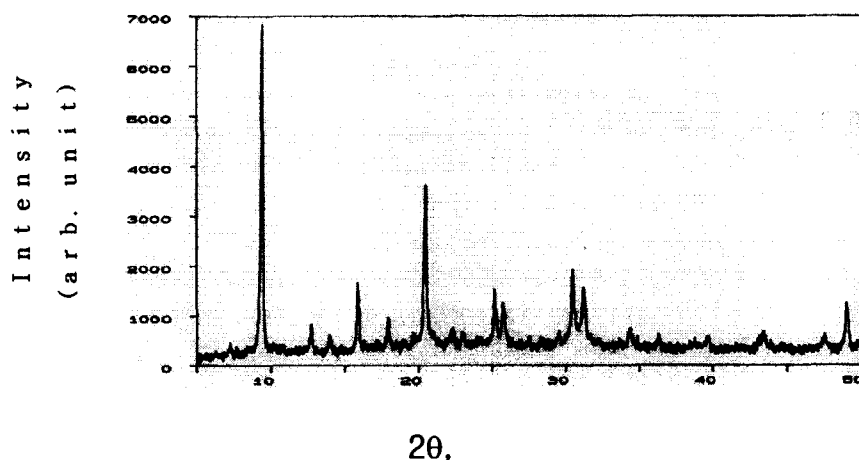


Fig. 1. X-ray powder diffraction pattern of as-synthesized MnH-SAPO-34.

ESR

Figs. 4 and 5 show the X-band ESR spectra of MnH-SAPO-34 samples ion exchanged in H₂O and methanol after various treatments. All signals split into 6 due to the hyperfine interaction with the Mn nucleus of Mn(II) ($S = 5/2$, $I = 5/2$) in the disordered systems which correspond to the transition between $|+1/2 \leftrightarrow |-1/2\rangle$.

Shoulders between the six hyperfines are apparent in all ESR signals with the exception of dehydrated MnH-SAPO-34. While the calcinations did not result in drastic changes of ESR spectrum, but rapid dehydration occurred at 400 °C. Some distinct features observed in the ESR signals of MnH-SAPO-34 during the dehydration process are followings; (1) a decrease in the A value of about 3 G is noted in all three samples, (2) dehydration at 400 °C of MnH-SAPO-34 ion-exchanged in de-ionized water results in a decrease in the intensity of ESR signals by a factor of 10, (3) the superposition of a broad background signal is observed but the shoulder in the dehydrated sample disappear (See Fig. 4 d). The broadening of the ESR signal implies the Mn(II) ions are no longer isolated from one another. A similar type of ESR signal broadening was reported for MnAPO-5 where Mn(II) ions are found to occupy extra-framework positions even at very low Mn(II) contents.⁷ This type of Mn(II) ESR signal is attributed to an increase of spin exchange due to a decrease into the distance between the Mn(II) ions upon dehydration.

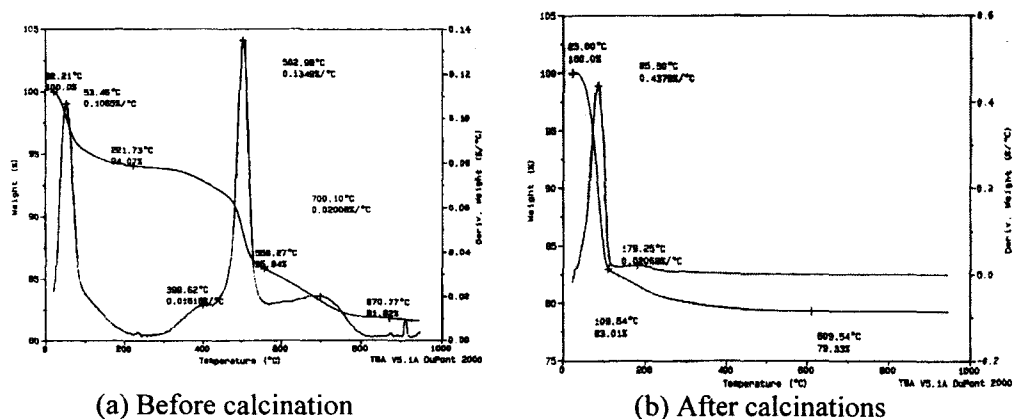


Fig. 2. TGA (Thermogravimetric Analysis) spectra of as-synthesized SAPO-34 (a) and calcined MnH-SAPO-34 (b).

We attempted to reproduce the features of this spectrum by computer simulations involving a superposition of two spectra. The simulation were done using the program given in EPR and included only the $M_s \mid -1/2 \rightarrow +1/2 \rangle$ transitions. This background is absent in the calculated spectra since only the $\mid -1/2 \rangle \rightarrow \mid +1/2 \rangle$ transitions were considered (See Fig. 6). All attempts to reproduce the spectrum using one species were failed. The main difficulty was to get the sharp features. Introducing a $E \neq 0$, namely a non-axial zero field tensor, did not introduce the sharp features. The relative intensities of the sharp peaks within a series of dehydrated samples were varied, which can supports the existence of two Mn(II).

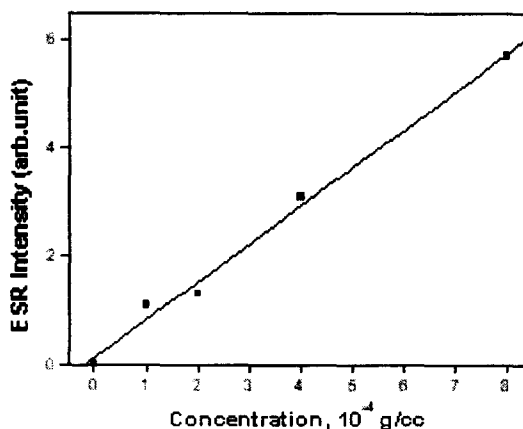


Fig. 3. Signal intensity of Mn(II) ion by double integration of ESR spectrum.

ESEM

All three samples are equilibrated with D₂O after (1) room temperature evacuation and (2) dehydration at 600 °C for 2 h. The deuterium modulation obtained at room temperature for MnH-SAPO-34 and dehydrated ones at 600 °C for 2 h and then exposed to D₂O are illustrated in Fig. 7.

Simulation of the deuterium modulation pattern suggests that two water molecules are coordinated to the Mn(II) ion in MnH-SAPO-34 ion-exchanged in de-ionized water, Mn²⁺-(H₂O)₂, situated at a distance (Mn²⁺-D)₄ of 0.31 nm with A_{iso} = 0.19 MHz, while three water molecules are coordinated to the Mn(II) ion in MnH-SAPO-34 ion-exchanged in MeOH, Mn²⁺-(H₂O)₃, situated at a distance (Mn²⁺-D) of 0.28 nm with A_{iso} = 0.21 MHz. The three-pulse ESEM spectrum obtained for (W)MnH-SAPO-34 after CH₃OD adsorption was simulated with two deuteriums interacting with Mn²⁺ at a distance of 0.29 nm with A_{iso} = 0.01 MHz, [Mn²⁺-(MeOH)₂], while three methanol molecules are coordinated to the Mn(II) ion in (M)MnH-SAPO-34, situated at a distance (Mn²⁺-D) of 0.29 nm with A_{iso} = 0.05 MHz (see Fig. 8). Fig. 9 shows the three-pulse ESE modulation of MnH-SAPO-34 with adsorbed CD₃OH. In this case, Mn²⁺ in (W)MnH-SAPO-34 interacts with six deuteriums, i.e., two molecules of methanol, situated at a distance (Mn²⁺-D) at 0.36 nm with an isotropic hyperfine coupling of 0.01 MHz, while Mn²⁺ in (M)MnH-SAPO-34 interacts with nine deuteriums, i.e., three molecules of methanol, at 0.35 nm with an isotropic hyperfine coupling of 0.04 MHz. Fig. 10 shows the three-pulse ESE modulation of MnH-SAPO-34 with adsorbed CH₃CH₂OD. The Mn²⁺ in (W)MnH-SAPO-34 and (M)MnH-SAPO-34 interacts with one deuterium, i.e., one molecule ethanol, at 0.32 and 0.31 nm with an

Table 1. ESR parameters of Mn-SAPO-34 molecular sieves with adsorbed solvents at 77 K.

sample	g	A (G)
MnH-SAPO-34 ^a as-synthesized	2.02	89.6
MnH-SAPO-34 ^b as-synthesized	2.02	91.4
MnH-SAPO-34 ^a evacuated at room temperature	2.02	89.1
MnH-SAPO-34 ^b evacuated at room temperature	2.02	86.7
MnH-SAPO-34 ^a evacuated at 400 °C for 3 h	2.02	86.2
MnH-SAPO-34 ^a evacuated at 600 °C for 2 h and adsorption with MeOH for 10 min	2.02	86.5
MnH-SAPO-34 ^b evacuated at 600 °C for 2 h and adsorption with MeOH for 10 min	2.02	93.6
MnH-SAPO-34 ^a evacuated at 600 °C for 2 h and adsorption with D ₂ O for 30 min	2.02	98.0
MnH-SAPO-34 ^b evacuated at 600 °C for 2 h and adsorption with D ₂ O at 30 min	2.02	98.0

^aion-exchanged in de-ionized water, ^bion-exchanged in MeOH, ^cref.⁵ A: hyperfine splitting

hyperfine coupling of 0.05 and 0.10 MHz. The ESEM results are summarized in Table II.

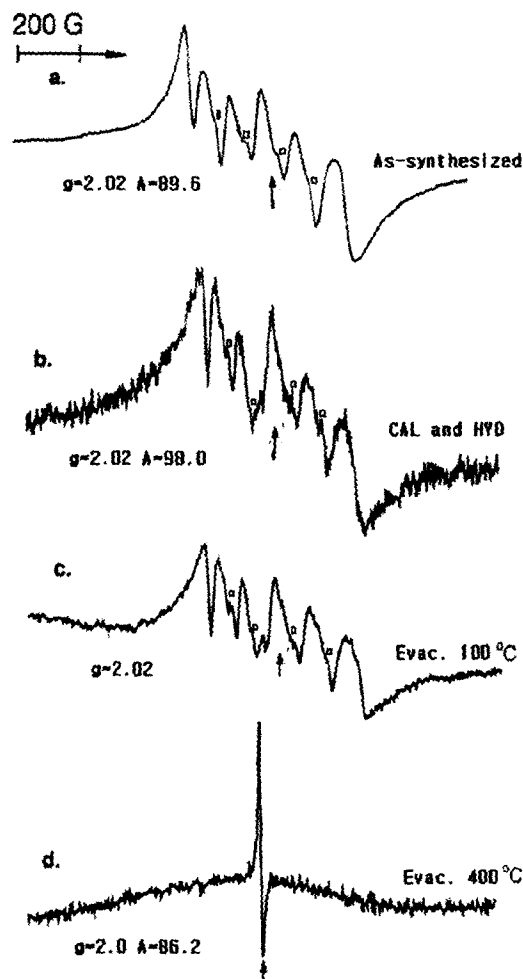


Fig. 4. ESR spectra of MnH-SAPO-34 molecular sieve at 77 K ion-exchanged in de-ionized water (a) as-synthesized MnH-SAPO-34 with 0.01 mol% manganese and (b) MnH-SAPO-34 with 0.01 mol% manganese calcined at 600 °C for 2 h and hydrated with D₂O at room temperature for 30 min and (c) MnH-SAPO-34 with 0.01 mol% manganese evacuated at 100 °C for 2 h and (d) MnH-SAPO-34 with 0.01 mol% manganese evacuated at 400 °C for 3 h. The four square indicate forbidden transitions.

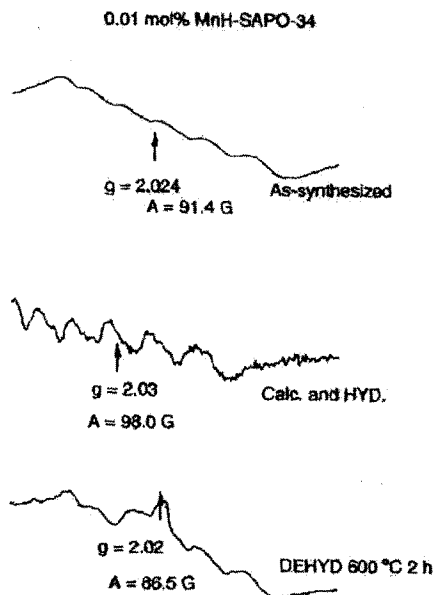


Fig. 5. ESR spectra recorded at 77 K of (a) as-synthesized MnH-SAPO-34 with 0.01 mol% ion-exchanged in Methanol and (b) MnH-SAPO-34 with 0.01 mol% manganese calcined at 600 °C for 2 h and hydrated with D₂O at room temperature for 30 min and (c) MnH-SAPO-34 with 0.01 mol% manganese dehydrated at 600 °C for 2 h.

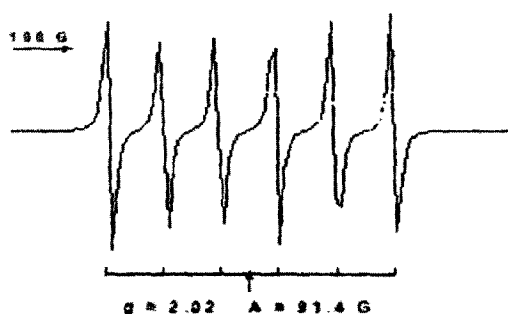


Fig. 6. Simulated ESR spectrum of MnH-SAPO-34 by using EPR program

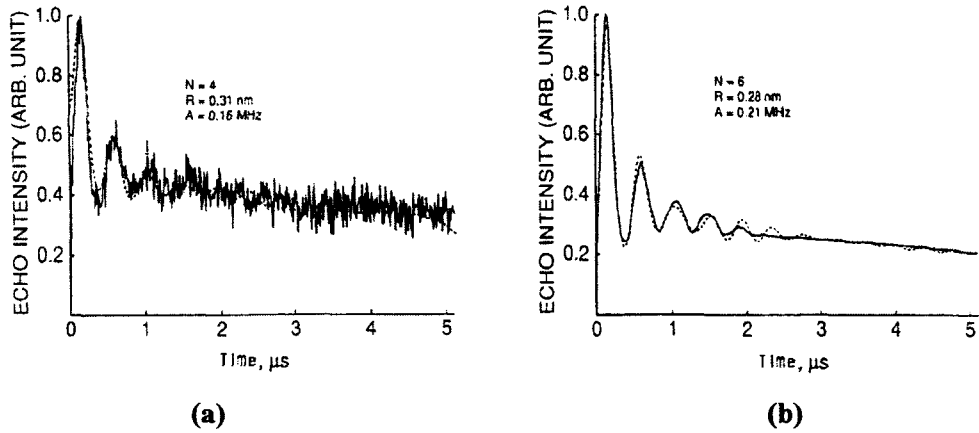


Fig.7. Experimental and simulated three-pulse ESEM of D_2O adsorbed MnH-SAPO-34(a : ion-exchanged in de-ionized water, b : Methanol) ; — ; experiment --- ; simulated.

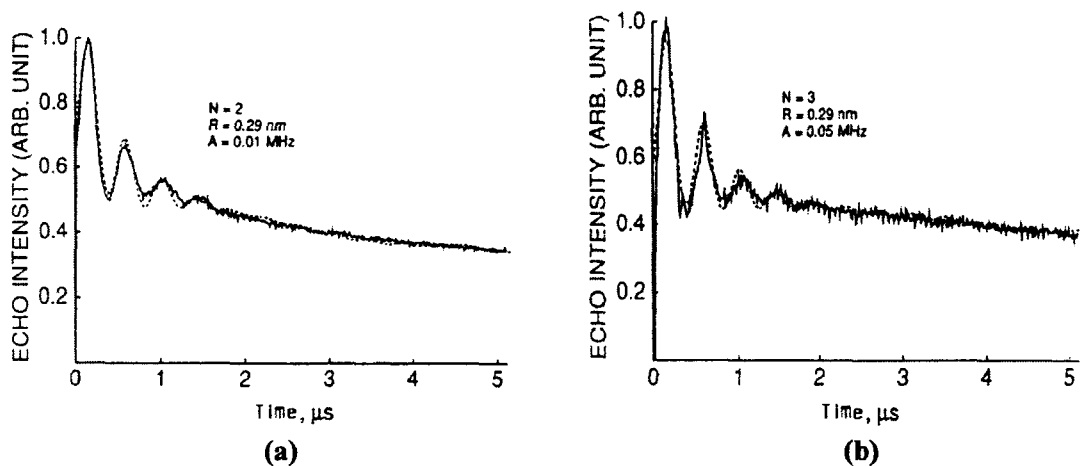


Fig. 8. Experimental and simulated three-pulse ESEM of CH_3OD adsorbed MnH-SAPO-34 (a: ion-exchanged in de-ionized water, b: Methanol) : — ; experimental --- ; simulated.

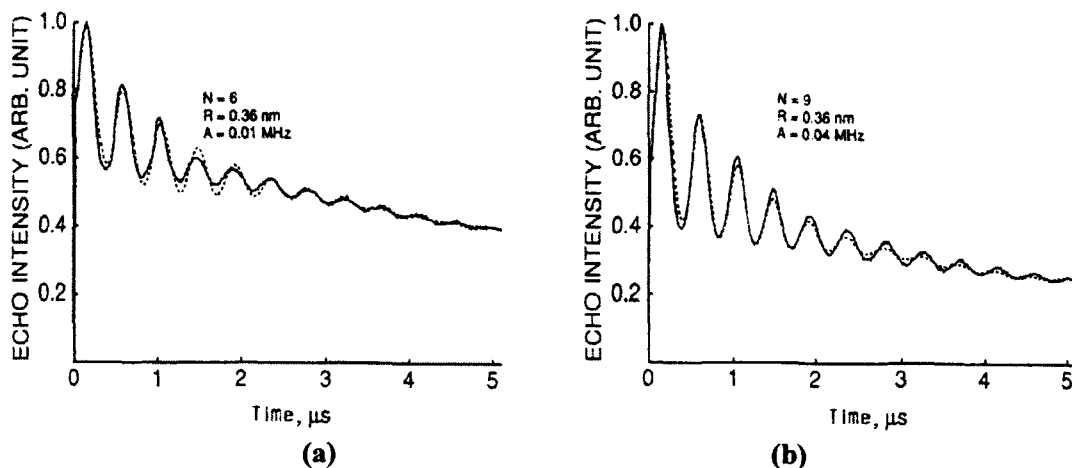


Fig. 9. Experimental and simulated three-pulse ESEM of CD₃OH adsorbed MnH-SAPO-34(a : ion-exchanged in de-ionized water, b : ion-exchanged Methanol) : — ; experimental - - ; simulated.

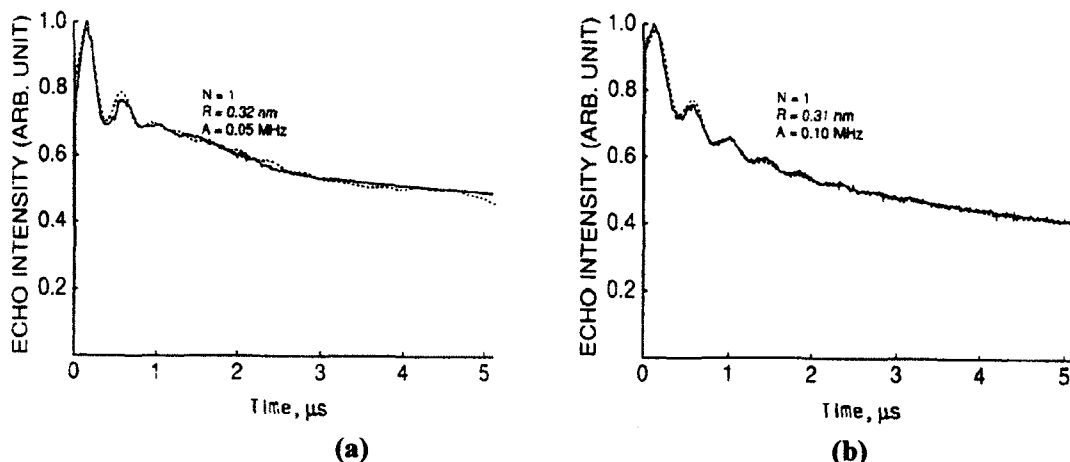


Fig. 10. Experimental and simulated three-pulse ESEM of CH₃CH₂OD adsorbed MnH-SAPO-34(a : ion-exchanged in de-ionized water, b : ion-exchanged Methanol) : — ; experimental --- ; simulated.

DISCUSSION

Several cation sites were identified in SAPO-34 and the possible locations of cation sites in SAPO-34 are shown in Fig. 11, by analogy with the cation sites of chabazite zeolite.⁹ site III is at the center of a hexagonal prism, site I is the center of a six-ring window, site I'

is the displaced from a six-ring into the cavity, and site IV is near the center of an eight-ring window. In zeolite chabazite, additional sites with low cation occupancy have also been reported.⁸

The presence of three different Mn species indicates that there are at least three possible different locations for Mn(II) ions in activated MnH-SAPO-34 molecular sieve. Djiengoue *et. al*⁹ also reported four sites for Ni(I) in NiH-SAPO-34 and suggested site IV as the most accessible, and site I as intermediately accessible and site III as the least accessible. Since the SAPO-34 sample analysed by electron probe microanalysis has a molar composition of Si_{0.11} Al_{10.55} P_{0.34}, there are 2-3 P nuclei, 3 Al nuclei, and 0-1 Si nuclei in a six-ring window of the framework. A six-ring window consisting of three phosphorus and three aluminum has no net framework charge. Therefore, it is likely that the positively charged manganese ion will locate near a negatively charged six-ring window with at least one silicon substitution for phosphorus. The behavior is similar to that in NiH-SAPO-34.⁹ This site can be identified as site I' in the chabazite cage near a six-ring window. (Fig. 11) However, the migration of metal ions from super cages and large channels to smaller ones during dehydration process is a common phenomenon in zeolites other molecular sieves.¹⁰ Similarly in SAPO-5 and SAPO-11, metal ions located initially in the large 12-ring or 10-ring channels migrate to smaller 6-ring channels during dehydration.¹¹ Since site I' is much more accessible site than site I, this means that manganese-exchanged SAPO-34 can be a good catalyst candidate.

Adsorbate Coordinate Structure

The ESR spectrum of as-synthesized MnH-SAPO-34 shows a hyperfine splitting of 89.6 G and is very similar to that of as-synthesized MnAPO-5⁷ and Mn-AlPO-11⁵ with comparable Mn contents. The Mn was found to be in extra-framework sites in MnAPO-5, while it was claimed to be incorporated into the framework in MnAPO-11. Accordingly, the ESR spectrum of the as-synthesized sample cannot provide any indication of framework substitution by itself. Calcination caused a increase in a hyperfine splitting to 98 G and the spectrum resembles very much to that of Mn(H₂O)₆²⁺. An increase in the hyperfine coupling constant after removal of the template is also observed in MnAPSO-44¹² and MnAPO-11.⁵ Thus, in the calcined samples, the Mn(II) is in an octahedral symmetry. The octahedral symmetry by itself does not contradict framework substitution since Mn as Al may coordinate two water molecule and this assumes a sixfold coordination states. Dehydration caused a significant decrease in a, 98 G to 86 G. Such a low hyperfine constant can be explained either by significant increase in a covalency of the bonding or alternatively by a change from octahedral to tetrahedral coordination.¹³ We prefer the second possibility according to that we proposed the following: Mn(II) is located in frame in the calcined hydrated state bound to four framework oxygens and to two water molecules. Removal of the water leaves tetrahedral Mn(II) coordinate to framework oxygen only. In MnAPO-5

dehydration of samples with similar Mn contents showed significant spin exchange⁷ indicating Mn(II) migration and in MnAPO-11 dehydration reduced a only to 87 G.¹⁴ The ESR and ESEM results show some significant differences for the coordination number between (W)MnH-SAPO-34 and (M)MnH-SAPO-34 with adsorbed D₂O and methanol. X-band ESR indicates that the spin-spin interaction is stronger in the impregnated sample suggesting the Mn(II) ions are closer to one another. Upon dehydration, X-band ESR spectrum of (W)MnH-SAPO-34 is still well resolved, while that of Mn(II) in (M)MnH shows a weak broad lines. This also shows that Mn(II) in (W)MnH-SAPO-34 is trapped in a site where the ions cannot move into closer proximity when water is removed from the structure which is expected if assuming Mn(II) is site I'.

Table II. Simulated parameters of three-pulse ESEM of Mn(II) in (W)MnH-SAPO-34 and (M)MnH-SAPO-34 treated with various adsorbates

sample	shell	N	R, nm	A, MHz
MnH-SAPO-34 ^a +D ₂ O	1	4	0.31	0.13
MnH-SAPO-34 ^b +D ₂ O	1	6	0.28	0.21
MnH-SAPO-34 ^a +CH ₃ OD	1	2	0.29	0.01
MnH-SAPO-34 ^b +CH ₃ OD	1	3	0.29	0.05
MnH-SAPO-34 ^a +CD ₃ OH	1	6	0.36	0.01
MnH-SAPO-34 ^b +CD ₃ OH	1	9	0.36	0.04
MnH-SAPO-34 ^a +CH ₃ CH ₂ OD	1	1	0.32	0.05
MnH-SAPO-34 ^b +CH ₃ CH ₂ OD	1	1	0.31	0.10

^aion-exchanged in de-ionized water, ^bion-exchanged in methanol media.

The simulation of the three-pulse ESEM signal obtained from MnH-SAPO-34 with adsorbed D₂O is inconsistent with a normal octahedral geometry of D₂O bonded to a transition metal cation in which the metal ion coordinates to the oxygen. Simulation of the deuterium modulation obtained from a 0.01 mol% (W)MnH-SAPO-34 sample with adsorbed D₂O suggests that the Mn(II) ions are coordinated to two water molecules. This other coordination number is also found for Mn(II) ions, prepared in a similar manner, in (M)MnH-SAPO-34.

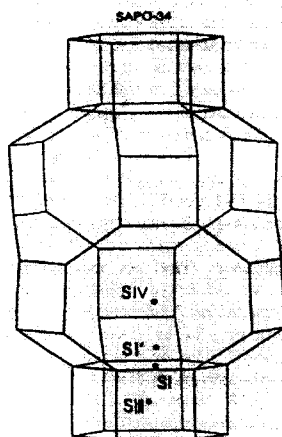


Fig. 11. Schematic representation of the unit cell of chabazite. Roman numerals indicate cation sites (adapted from ref 9).

In the present work, we suggest that the structure of as small SAPO-34 gives rise to the other adsorption coordination number as the ion-exchanged media. It is understandable that manganese ion in (M)MnH-SAPO-34 is locating to relatively exposed site IV because of relatively large Methanol molecule than relatively small water molecule(kinetic diameter: water 2.65 Å methanol 3.8 Å).¹⁵ Therefore, it is also considerable that location of manganese ion in (W)MnH-SAPO-34 is site I' that is placed from a six-ring into the cavity, while the location of manganese ion in (M)MnH-SAPO-34 is to site IV that is near the center of an eight-ring window.

CONCLUSION

This work shows the spectroscopic evidence that the location of manganese ion in MnH-SAPO-34 ion-exchanged in de-ionized water is different from that of manganese ion ion-exchanged in methanol, induced by the comparison of ESEM results ion-exchanged in de-ionized water with those in methanol. We suggest that manganese ion in (M)MnHSAPO-34 is locating to site IV relatively more exposed, while manganese ion in (W)MnH-SAPO-34 is locating in site I' relatively less exposed.

REFERENCE

1. S. T. Wilson, B. M. Lok, C. A. Messina, T. R. Cannan, and E. M. Flanigen, *J. Am.*

- Chem. Soc.*, **104**, 1146 (1982).
2. B. M. Lok, C. A. Messina, R. L. Patton, R. T. Gajek, T. R. Cannan, and E. M. Flanigen, *J. Am. Chem. Soc.*, **106**, 6092 (1984).
 3. R. Szostak, Molecular Sieves, *Principle of Synthesis and Identification*, Van Nostrand Reinhold; New York, 1989, Chap. 4.
 4. B. M. Lok, C. A. Messina, R. L. Patton, R. T. Gajek, T. R. Cannan, and E. M. Flanigen, U. S. Pat, 4400871, (1984) (b) B. M. Lok, C. A. Messina, R. L. Patton, R. T. Gajek, T. R. Cannan, and E. M. Flanigen, *J. Am. Chem. Soc.*, **106**, 6092 (1984).
 6. G. Brounet, X. Chen., C. W. Lee, and L. Kevan, *J. Am. Chem. Soc.*, **114**, 3720 (1992).
 7. Y. Xu, P. J. Maddox, and J. W. Couves, *J. Am. Chem. Soc.*, Faraday Trans., **86**, 425 (1990).
 8. Z. Levi, A. M., Raitsiming, and D. Goldfarb, *J. Phys. Chem.*, **95**, 7830 (1991).
 9. W. J., Mortier, *Compilation of Extra-framework sites in Zeolites; Structure Commission of the International Zeolite Association*: Butterworth: Survey, 1982; pp 11-12.
 10. M. Djieugoue, A. M. Prakash, and L. Kevan, *J. Phys. Chem.*, **102**, 4386 (1998).
 11. W. M. H. Sachtler, and Z. Zang, *Adv. Catal.*, **39**, 129 (1993).
 12. C. W. Lee, X. Chen, and L. Kavan, *Catal. Lett.*, **15**, 75 (1997).
 13. Z. Levi, D. Goldfarb, and J. Batisto, *J. Am. Chem. Soc.*, Submitted.
 14. J. Levanon, and Z. Luz, *J. Chem. Phys.*, **49**, 2031 (1968).
 15. G. Bronet, X. Chen, C. W. Lee, and L. Kevan, *J. Phys. Chem.*, **96**, 3110 (1992).
 16. R. Szostark, Molecular Sieves: *Principle of Synthesis and Identification*, Van Nostrand Reinhold; New York, 1989, Chap.1, pp 18.
 17. Kevan, L. In *Time Domain Electron Spin Resonance*; L. Kevan, and R. N. Schwartz, Eds.; Wiley: New York, 1979, Chap. 8.